

2018

Simulation of the Superheated Water Expansion Process in a Cylinder with Moving Piston

Qi Wang

XI'AN JIAOTONG UNIVERSITY, China, People's Republic of, 1175358231@qq.com

Zhao Zhang

Xi'an Jiaotong University, China, People's Republic of China, zhangzhaoxjtu@163.com

Weifeng Wu

XI'AN JIAOTONG UNIVERSITY, China, People's Republic of, 35748093@qq.com

Follow this and additional works at: <https://docs.lib.purdue.edu/icec>

Wang, Qi; Zhang, Zhao; and Wu, Weifeng, "Simulation of the Superheated Water Expansion Process in a Cylinder with Moving Piston" (2018). *International Compressor Engineering Conference*. Paper 2563.

<https://docs.lib.purdue.edu/icec/2563>

This document has been made available through Purdue e-Pubs, a service of the Purdue University Libraries. Please contact epubs@purdue.edu for additional information.

Complete proceedings may be acquired in print and on CD-ROM directly from the Ray W. Herrick Laboratories at <https://engineering.purdue.edu/Herrick/Events/orderlit.html>

Simulation of the Superheated Water Expansion Process in a Cylinder with Moving Piston

QI WANG, ZHAO ZHANG, WEIFENG WU*

School of Energy and Power Engineering, Xi'an Jiaotong University
Xi'an, Shaanxi, China
Tel: +86-29-82665526, E-mail: weifengwu@xjtu.edu.cn

*Corresponding Author

ABSTRACT

The Trilateral Cycle has attracted more and more attentions because of its better temperature profiles matching in the heater compared to conventional heat recovery cycles, such as the Organic Rankine Cycle and the Kalina Cycle. However, the actual fundamentals of the two-phase expansion process have not been clarified, especially, the evolution mechanisms of the evaporating rate and the degree of superheat during the expansion process are indistinct. In the present study, two-phase expansion process of superheated water in a cylinder with moving piston was analyzed. A model was proposed to calculate the evaporating rate and the degree of superheat of liquid water. A semiempirical Nusselt number was adopted to solve the energy conservation equations. It was shown that the degree of superheat of liquid water was increased rapidly to the maximum at the beginning of the expansion process and then was decreased continuously. The degree of superheat was almost equal to 0 at the end of the expansion process. The simulation results also showed a complex evolution profile of the evaporating rate during the expansion process. As a whole, the evaporating rate was increased from 0 to the maximum, and then it was decreased to 0 at the end of the expansion process. This situation is similar to the experimental results in the published literature. The evaporating rate appeared a transient dropping process at the beginning of the expansion. It was considered that this result was associated with the rapid decline of the degree of superheat. Meanwhile, there were two or three significant inflection points on the evolution profile. From the model prediction, it was considered that the injection process of the saturated liquid water would have an influence on the degree of superheat of liquid water, and the evaporating rate may be related to the degree of superheat of liquid water, the piston velocity and the mass of liquid water of the expansion process.

1. INTRODUCTION

With the rapid development of energy economy, the ongoing increase of energy demands and the continuous reduction of energy reserves have become a pair of contradictions between provision and requirement, constraining the development of social economy. It is becoming more and more important for humans to make rational and efficient use of energy, especially for low-to-moderate temperature waste heat sources. There are three outstanding waste heat recovery cycles known in the field of moderate to low grade heat recovery and utilization: the Organic Rankine Cycle (ORC), the Kalina Cycle and the Trilateral Cycle (TLC).

Several authors compared the performance of these cycles from the viewpoint of efficiency, including exergy efficiency and thermal efficiency. Yari *et al.* (2015) made a comparison of the performance of the TLC, the ORC and the Kalina Cycle. It was found that when a low grade heat source was used for these three systems, the TLC showed great potential of achieving a higher net output power, and the net output power was increased with the increase of the expander inlet temperature. While, the product cost for the TLC plant was decreased. Fischer (2011) compared the optimized ORC-systems with organic working fluids and the optimized TLC-systems using liquid water as working fluid, and found that the exergy efficiency for power production was higher by 14%-29% for the TLC than for the ORC. Lai and Fischer (2012) compared the TLC (using water as working fluid) with the ORCs (using different working fluids) and water Clausius Rankine cycles, and reported that the Power Flash Cycle (PFC) had a larger power production efficiency than the ORCs but greater volume flows at the expander exit. It was also reported

that TLC-systems with water as working fluid had the highest or nearly highest efficiency for power production in all cases.

It could be seen from these analysis that the efficiency of the TLC can be theoretically the highest or nearly highest among other heat recovery cycles and the two-phase expansion process in the cylinder is one of the key links in a TLC-system. There are several researches about wet-vapor expansion in a reciprocating expander. Kanno and Shikazono (2015) conducted an experimental study on two-phase expansion process in a cylinder with moving piston and proposed a model to predict pressure change in this process. It was found that the temperature distribution of liquid phase in the cylinder was the key factor for affecting the adiabatic efficiency. Steffen *et al.* (2013) came up with a novel TLC using a cyclone separator, and presented a theoretical method to calculate isentropic efficiency of the reciprocating expander. Meanwhile, various working fluids were investigated, and it was concluded that when water was used as working fluid, the isentropic efficiency was in the range of 0.75-0.88 and dropped significantly for high engine speeds and stroke volumes. It was also pointed out that the injection mass had the greatest influence on the isentropic efficiency, because it impacted dead volume and injection performance.

However, the actual fundamentals of the two-phase expansion process have not been clarified, especially, the evolution mechanisms of the evaporating rate and the degree of superheat during the expansion process are indistinct. Therefore, it is very vital to clarify the two-phase expansion process in the cylinder for obtaining a reliable isentropic efficiency of the two-phase expander. In the present study, two-phase expansion process of superheated water in a cylinder with moving piston was analyzed and a model was proposed to calculate the evaporating rate and the degree of superheat of liquid water.

2. DESCRIPTION OF THE SIMPLE TLC AND THE EXPANSION MODEL USED IN THE SIMULATION

2.1. Description of the simple TLC

The simple TLC consists of four key components, which are the pump, the heater, the two-phase expander and the condenser. Figure 1 shows the schematic cycle configuration and the T-s diagram of the simple TLC.

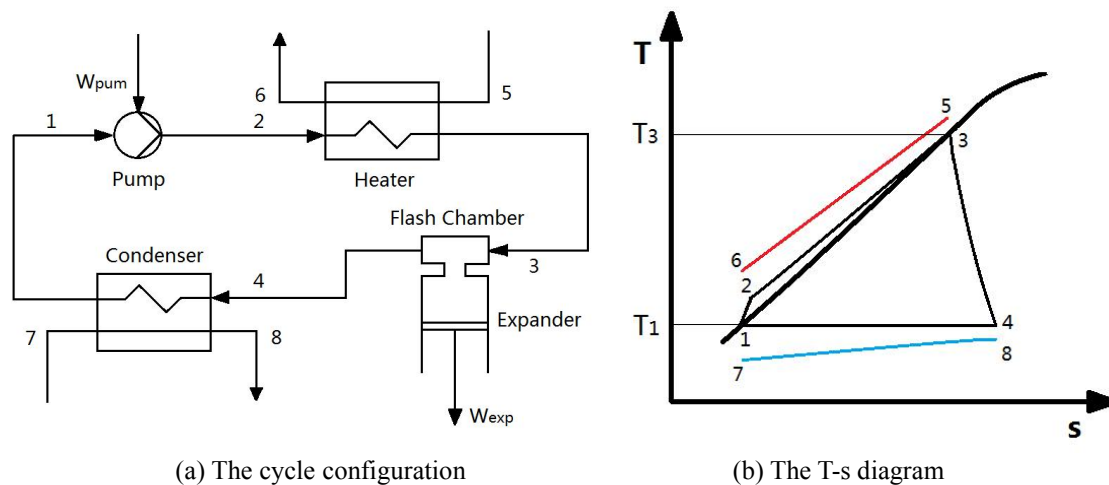


Figure 1: The schematic cycle configuration and the T-s diagram of the simple TLC

In such a configuration, the working fluid at state 1 is a saturated liquid water with temperature T_1 at the vapor pressure p_1 . Then the low pressure saturated liquid at the condenser exit is pumped to the heater and the pressure of the liquid is increased by the pump to pressure p_2 at state 2. Thereafter, the liquid water is heated up just to its saturated temperature (boiling point) at constant pressure p_2 . The saturated liquid water at state 3 is rapidly injected into the flash chamber which is part of the expander, and then it is flashed continuously till it arrives at state 4 with temperature T_1 and vapor quality x . Meanwhile, the pressure of the working fluid drops quickly during this expansion process and eventually reduces to pressure p_4 . In state 4, the working fluid is the two-phase mixture (the

wet vapor) which comprises saturated liquid water and saturated vapor, and it is discharged from the expander. Lastly, the exhausted wet vapor is condensed in the condenser till it reaches state 1 to start the new cycle. The heat carrier supplying the heat to the TLC-system enters the heater at temperature T_5 and leaves it at temperature T_6 . At the same time, the cooling agent removing the heat from the TLC-system enters the condenser at temperature T_7 and leaves it at temperature T_8 .

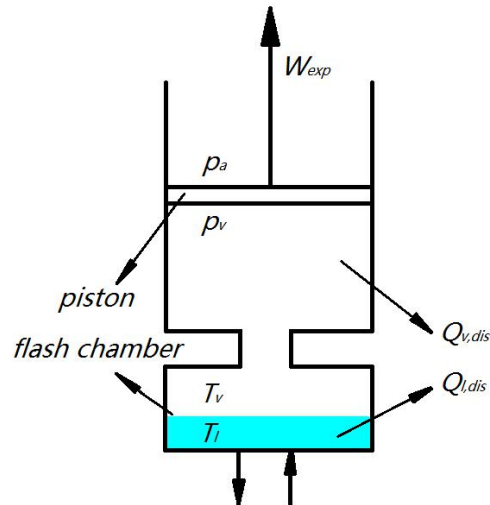


Figure 2: The expansion model used in the simulation

2.2. The expansion model used in the simulation

The expansion model used in the simulation is shown in Figure 2. In Figure 2, the flash chamber is a small volume providing phase separation of vapor and liquid, allowing the vapor flow into the cylinder and avoiding the hydraulic shocks in the cylinder. However, this chamber will form dead volume and keep a part of working fluid of the former cycle, which is named residual mass. The residual mass and the dead volume are expressed as Eqs. (1) and (2) respectively. Here, a and k are the coefficients, and $\rho_l(T_{inj})$ is the liquid water density which corresponds to the injection temperature T_{inj} .

$$m_{res} = a \cdot m_{inj,tot} \quad (1)$$

$$V_d = k \cdot \frac{m_{res} + m_{inj,tot}}{\rho_l(T_{inj})} \quad (2)$$

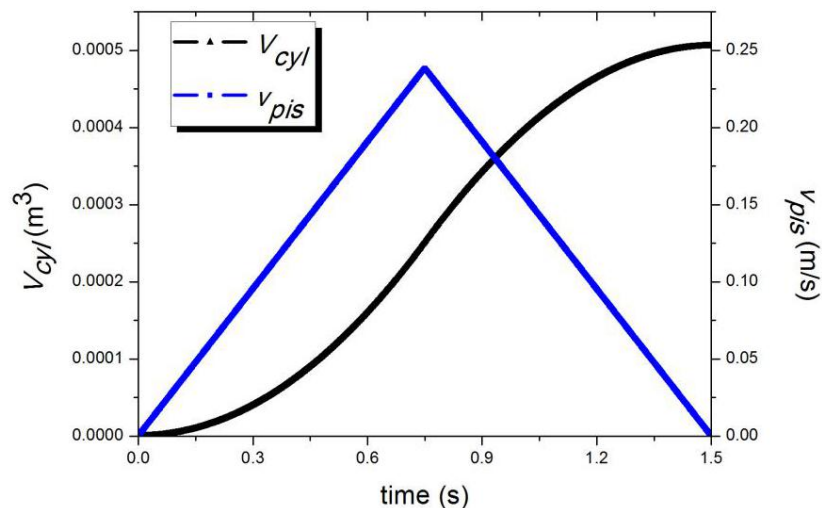


Figure 3: Velocity change of the piston and volume change of the cylinder

In order to compare with the results of the published literature (Kanno and Shikazono, 2016), in this paper, it is assumed that the piston performs a simple uniform variable speed motion. The diameter of piston, d_{pis} , is 0.06 m and the constant acceleration of piston, a , is ± 0.318 m/s². The saturated liquid water with a temperature of 473.15 K is injected into the flash chamber rapidly. As the piston moves, the vapor pressure in the cylinder declines, causing the saturated water be changed into superheated water. Then, the superheated water is flashed and generates vapor. The generated vapor is expanded in the cylinder and pushes the piston. During the expansion process, temperature and pressure of the working fluid are decreased. When the piston reaches the dead point, where the volume of the cylinder is the biggest and equals to the stroke volume, the two-phase expansion process is finished. Finally, the vapor-liquid two-phase mixture (the wet vapor) is discharged from the cylinder and the flash chamber.

Table 1: Operating parameters used in the simulation

Parameters	Values	Units
T_{inj} or T_3	473.15	[K]
T_4	428.15	[K]
p_a	101.325	[kPa]
$m_{inj,tot}$	0.015	[kg]
n	20	[r/min]
a	0.05	[no.]
k	3	[no.]
α	± 0.318	[m/s ²]
d_{pis}	0.06	[m]
d_{inj}	0.005	[m]
v_{inj}	5	[m/s]
z	1	[no.]
V_{str}	5.06×10^{-4}	[m ³]
V_d	5.46×10^{-5}	[m ³]

The operating parameters used in the simulation is shown in Table 1. During the expansion process, velocity change of the piston and volume change of the cylinder are shown in Figure 3.

3. MODELING OF THE TWO-PHASE EXPANSION PROCESS

During the two-phase expansion process, the mass balance equations in the cylinder are calculated by Eqs. (3-6).

$$m = m_{res} + m_{inj} = m_l + m_v \quad (3)$$

$$\frac{dm_l}{dt} + \frac{dm_v}{dt} = \frac{dm_{inj}}{dt} \quad (4)$$

$$V = V_{cyl} + V_d = V_l + V_v \quad (5)$$

$$V_{cyl} = \int_0^t A_{pis} \cdot v_{pis} dt \quad (6)$$

Based on the analysis of the two-phase expansion process in the published literature (Kanno and Shikazono, 2017), it was considered that the heat transfer between the gas-liquid interface and the bulk liquid was the predominant mechanism of the two-phase expansion, as shown in Eq. (7).

$$\frac{dm_v}{dt} \cdot L = A_{pis} h_{int} (T_l - T_v) \quad (7)$$

The energy balance equations for the liquid and the vapor are expressed as Eqs. (8) and (9) respectively.

$$(m_l + dm_l)u_l' = m_l u_l - dm_v u_{v,fla} + dm_{inj} u_{l,inj} - dQ_{l,dis} \quad (8)$$

$$(m_v + dm_v)u'_v = m_v u_v + dm_v u_{v,fla} - dQ_{v,dis} - p_v dV + dW_{com} \quad (9)$$

$$dW_{com} = p_v \frac{dm_v}{\rho_v} \quad (10)$$

In Eq. (8), u'_l is defined as the specific internal energy of liquid water in the latter time step and $Q_{l,dis}$ is the liquid heat dissipation which can be obtained from the calibration experiment (Kanno and Shikazono, 2015). Similarly, u'_v in Eq. (9) is defined as the specific internal energy of vapor in the latter time step and $Q_{v,dis}$ is the vapor heat dissipation which can be obtained from the calibration experiment (Kanno and Shikazono, 2016). In Eq. (9), the compression work, dW_{com} , caused by the generation of the flash vapor, is calculated by Eq. (10). Here, when the time step, dt , is set as a small enough value, the vapor pressure p_v can be considered as a constant in this time step. To solve the energy conservation equations, the semiempirical Nusselt number obtained by the dimensional analysis in the literature (Kanno and Shikazono, 2017) was used in this study, as shown in Eq. (11).

$$\begin{aligned} Nu &= \frac{h_{int} l_{Lap}}{\lambda_l} \\ &= 1 + c_1 \left(\frac{Cp_l \mu_l}{\lambda_l} \right)^{c_2} \left(\frac{\rho_l v_{pis} l_{Lap}}{\mu_l} \right)^{c_3} \left(\frac{\rho_v}{\rho_l} \right)^{c_4} \left(\frac{d_b}{l_{Lap}} \right)^{c_5} \\ &= 1 + c_1 \text{Pr}^{c_2} \text{Re}^{c_3} \left(\frac{\rho_v}{\rho_l} \right)^{c_4} \left(\frac{d_b}{l_{Lap}} \right)^{c_5} \end{aligned} \quad (11)$$

$$c_1 = 18.2 \quad c_2 = 0.58 \quad c_3 = 0.987 \quad c_4 = 0.77 \quad c_5 = -0.40$$

There are some operating parameters and thermophysical properties related to the flash evaporation phenomenon, including Laplace length, l_{Lap} , departure bubble diameter, d_b , vapor velocity at the vapor-liquid interface, $v_{v,int}$, vapor density, ρ_v , liquid density, ρ_l , liquid heat capacity, Cp_l , and liquid thermal conductivity, λ_l . In Eq. (11), l_{Lap} is widely used as a characteristic length in pool boiling, which is expressed as Eq. (12). From the Cole's correlation, d_b is calculated, as shown in Eqs. (11) and (13). The Jacob number in Eq. (14) is the ratio of sensible heat to latent heat absorbed during the vapor-liquid phase change, and is defined as Eq. (15).

$$l_{Lap} = \sqrt{\frac{\sigma_l}{g(\rho_l - \rho_v)}} \quad (12)$$

$$Bo = \frac{d_b^2 g(\rho_l - \rho_v)}{\sigma_l} \quad (13)$$

$$Bo^{\frac{1}{2}} = 0.04 Ja \quad (14)$$

$$Ja = \frac{\rho_l Cp_l (T_l - T_{sat}(p_v))}{\rho_v L} \quad (15)$$

Here, the temperature $T_{sat}(p_v)$ is the saturation temperature which corresponds to the vapor pressure in the cylinder. The evaporating rate, γ , and the degree of superheat of liquid water of the expansion process, ζ , are defined as Eqs. (16) and (17) respectively. Lastly, it should be pointed out that the thermophysical properties involved in the above equations are obtained by using the REFPROP software.

$$\gamma = \frac{dm_v}{dt} \quad (16)$$

$$\zeta = T_l - T_{sat}(p_v) \quad (17)$$

4. RESULTS AND DISCUSSION

4.1. Temperature evolution and pressure evolution of the two-phase expansion process

Figure 4 shows the temperature evolution curve and the pressure evolution curve of the expansion process. It can be seen from the Figure 4 that the pressure in the cylinder and the temperature of the working fluid (including water and vapor) have similar evolution processes during the two-phase expansion. All of them rise rapidly at the beginning of the expansion process, reaching the highest point, and then declining continuously till the expansion process is finished.

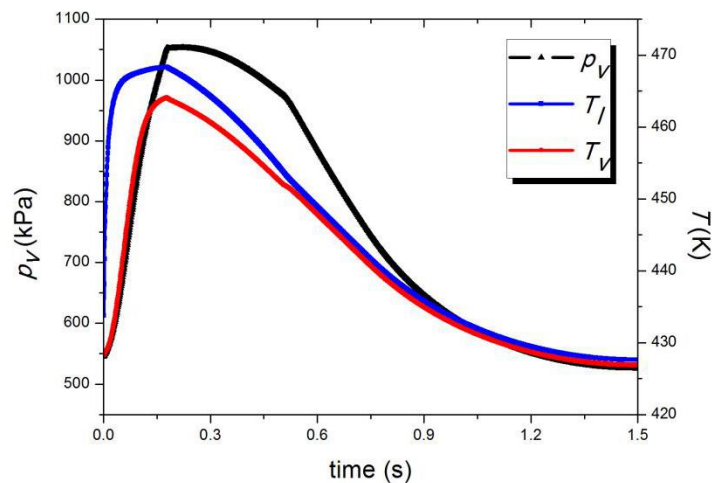


Figure 4: Temperature evolution and pressure evolution curves of the expansion process

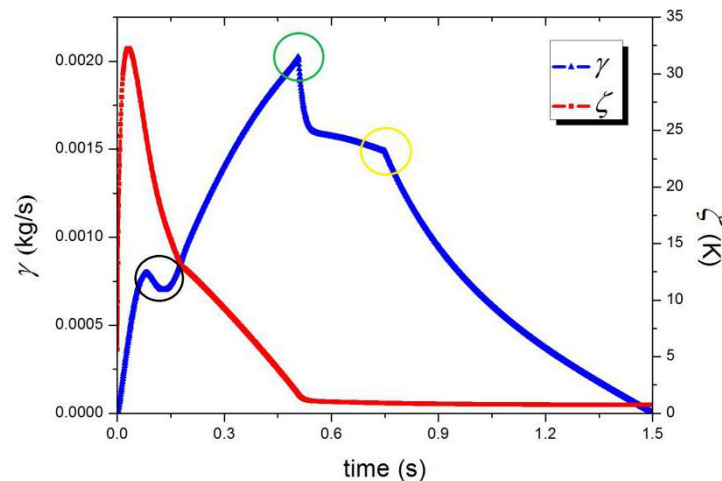
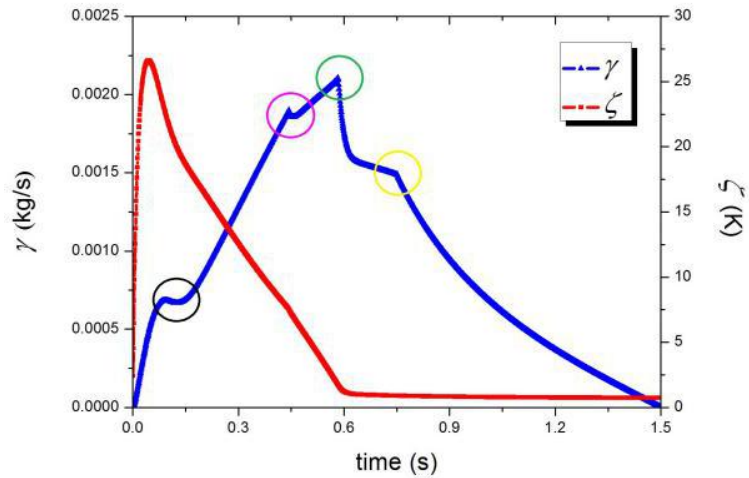


Figure 5: Evaporating rate and the degree of superheat of liquid water of the expansion process

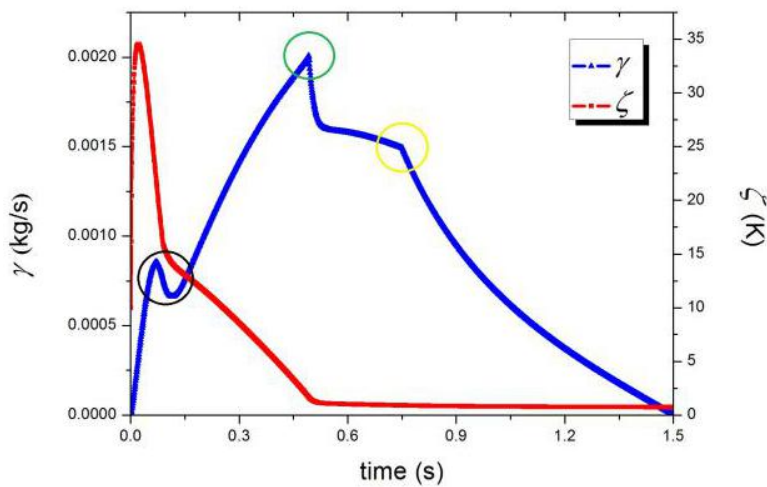
4.2. Evaporating rate and degree of superheat of liquid water

The evaporating rate and the degree of superheat of liquid water of the expansion process are shown in Figure 5. In Figure 5, it can be seen that the degree of superheat of liquid water is increased rapidly to the maximum (about 32 K) at the beginning of the expansion process and then is decreased continuously. The degree of superheat is almost equal to 0 at the end of the expansion process. The simulation results in Figure 5 also show a complex evolution profile of the evaporating rate during the expansion process. As a whole, the evaporating rate is increased from 0 to the maximum, and then it is decreased to 0 at the end of the expansion process. It is noticed that this situation is similar to the experimental results in the published literature (Kanno and Shikazono, 2017). However, it is found that the evaporating rate appears a transient dropping process at the beginning of the expansion which is marked with the black circle, and then the evaporating rate is increased again and reaches the highest point which is marked with the green circle, as shown in Figure 5. It was considered that the occurrence of this transient dropping process was

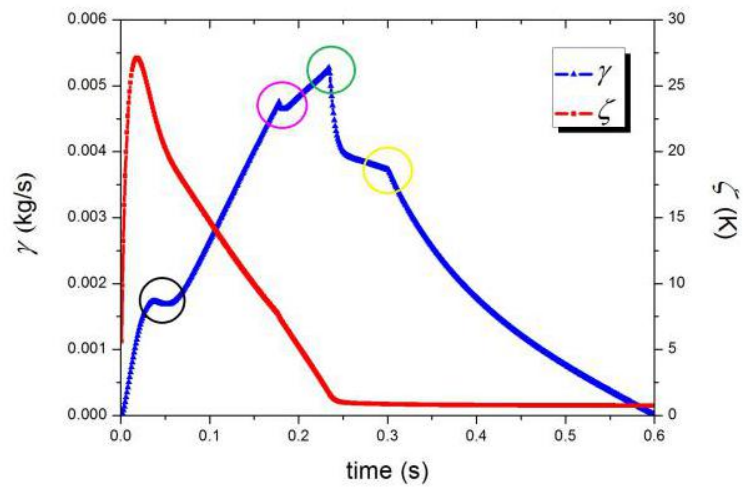
associated with the rapid decline of the degree of superheat of liquid water, and the occurrence of the highest point of the evaporating rate was caused by the small degree of superheat of liquid water which is almost equal to 0. Meanwhile, in Figure 5, a significant inflection point marked with the yellow circle appears at the middle of the evolution profile of the evaporating rate, where the velocity of piston is the biggest. It was considered that the inflection point marked with the yellow circle may be related to the velocity of piston.



(a)



(b)



(c)

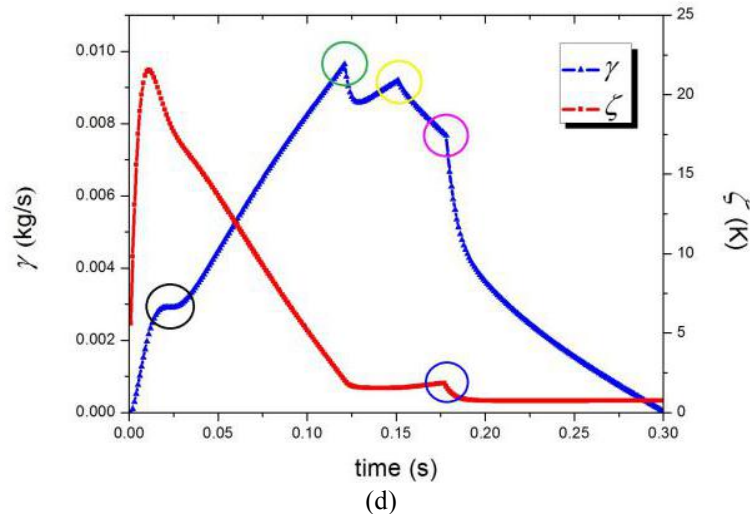
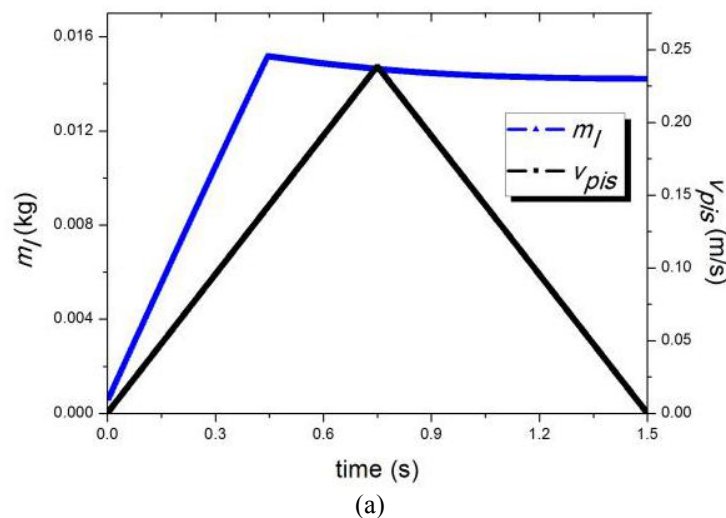


Figure 6: Evaporating rate and the degree of superheat of the expansion process under four different operating conditions: (a) $n = 20$ r/min, $v_{inj} = 2$ m/s, $\alpha = \pm 0.318$ m/s²; (b) $n = 20$ r/min, $v_{inj} = 10$ m/s, $\alpha = \pm 0.318$ m/s²; (c) $n = 50$ r/min, $v_{inj} = 5$ m/s, $\alpha = \pm 1.988$ m/s²; (d) $n = 100$ r/min, $v_{inj} = 5$ m/s, $\alpha = \pm 7.950$ m/s²

In order to verify our guess, the simulation results under four different operating conditions are analyzed. The expander speed, n , the injection speed, v_{inj} , and the acceleration of piston, α , are changed, while other operating parameters remain unchanged. The evaporating rate and the degree of superheat of liquid water of the expansion process under these operating conditions are shown in Figure 6. The mass of liquid water and the piston velocity of the expansion process under these operating conditions are shown in Figure 7. Based on the simulation results, it can be seen that the evolution processes of the evaporating rate and the degree of superheat of liquid water are similar to the previous situation. As is shown in Figure 5, the transient dropping process of the evaporating rate at the beginning of the expansion and the two inflection points appearing at the evolution profile of the evaporating rate exist in all cases. It is also found that, in Figure 6a, c and d, there is another inflection point existing at the evolution profile of the evaporating rate, which is marked with the pink circle. After comparing Figure 6 with Figure 7, it was considered that this point may be related to the mass of liquid water of the expansion process. Meanwhile, it can be seen from Figure 6d that a significant inflection point marked with the blue circle appears at the evolution profile of the degree of superheat of liquid water, where the injection process of the saturated liquid water is finished and the mass of liquid water is the biggest. It was considered that the injection process of the saturated liquid water would have an influence on the degree of superheat of liquid water, and the degree of superheat of liquid water would have an impact on the evaporating rate.



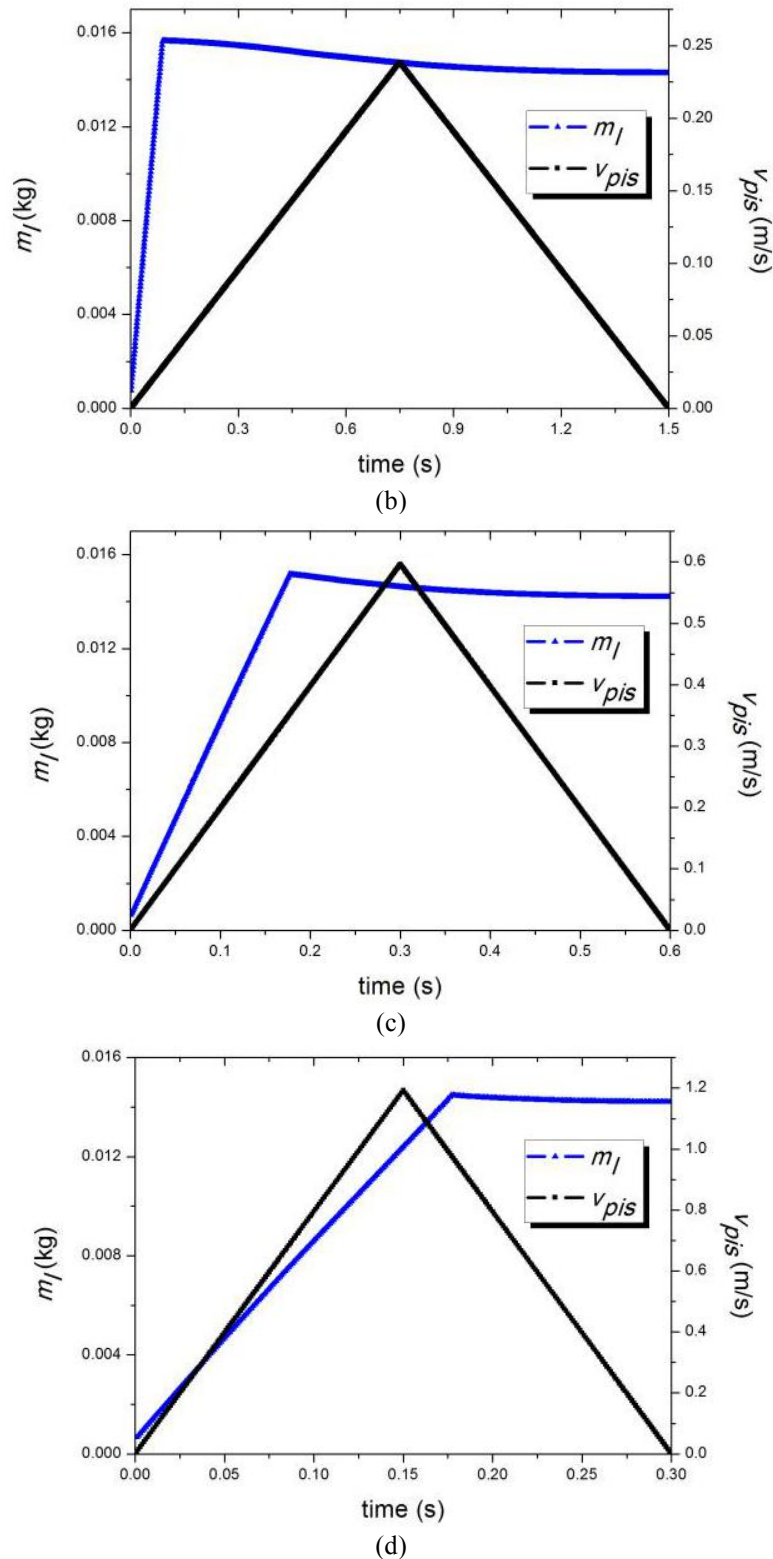


Figure 7: Mass of liquid water and the piston velocity of the expansion process under four different operating conditions: (a) $n = 20$ r/min, $v_{inj} = 2$ m/s, $\alpha = \pm 0.318$ m/s²; (b) $n = 20$ r/min, $v_{inj} = 10$ m/s, $\alpha = \pm 0.318$ m/s²; (c) $n = 50$ r/min, $v_{inj} = 5$ m/s, $\alpha = \pm 1.988$ m/s²; (d) $n = 100$ r/min, $v_{inj} = 5$ m/s, $\alpha = \pm 7.950$ m/s²

5. CONCLUSIONS

In the present study, two-phase expansion process of superheated water in a cylinder with moving piston was analyzed and a model was proposed to calculate the evaporating rate and the degree of superheat of liquid water. Following conclusions could be obtained.

- The degree of superheat of liquid water was increased rapidly to the maximum at the beginning of the expansion process and then was decreased continuously. The degree of superheat was almost equal to 0 at the end of the expansion process.
- The evolution profile of the evaporating rate during the expansion process was complicated. As a whole, the evaporating rate was increased from 0 to the maximum, and then it was decreased to 0 at the end of the expansion process. However, the evaporating rate appeared a transient dropping process at the beginning of the expansion, and it was considered to be associated with the rapid decline of the degree of superheat of liquid water. Meanwhile, there were two or three significant inflection points on this evolution profile.
- From the model prediction, it was considered that the injection process of the saturated liquid water would have an influence on the degree of superheat of liquid water, and the evaporating rate may be related to the degree of superheat of liquid water, the piston velocity and the mass of liquid water of the expansion process.

NOMENCLATURE

a	residual mass coefficient	(-)	L	latent heat	(J/kg)
A	area	(m ²)	s	entropy	(J/K)
k	dead volume coefficient	(-)	u	specific internal energy	(J/kg)
l	length	(m)	x	vapor quality	(-)

Subscripts

a	atmosphere	l	liquid
b	bubble	Lap	laplace
com	compression	pis	piston
cyl	cylinder	pum	pump
d	dead	res	residual
dis	dissipation	str	stroke
fla	flash	sat	saturation
inj	injection	tot	total
int	interface	v	vapor

REFERENCES

- H. Kanno & N. Shikazono. (2015). Experimental and modeling study on adiabatic two-phase expansion in a cylinder. *Int. J. Heat Mass Transf.*, 86, 755-763.
- H. Kanno & N. Shikazono. (2016). Experimental study on two-phase adiabatic expansion in a reciprocating expander with intake and exhaust processes. *Int. J. Heat Mass Transf.*, 102, 1004-1011.
- H. Kanno & N. Shikazono. (2017). Modeling study on two-phase adiabatic expansion in a reciprocating expander. *Int. J. Heat Mass Transf.*, 104, 142-148.
- J. Fischer. (2011). Comparison of trilateral cycles and organic Rankine cycles. *Energy*, 36(10), 6208-6219.
- M. Steffen, M. Löffler & K. Schaber. (2013). Efficiency of a new Triangle Cycle with flash evaporation in a piston engine. *Energy*, 57, 295-307.
- M. Yari, A.S. Mehr, V. Zare, S.M.S. Mahmoudi & M.A. Rosen. (2015). Exergoeconomic comparison of TLC (trilateral Rankine cycle), ORC (organic Rankine cycle) and Kalina cycle using a low grade heat source. *Energy*, 83, 712-722.
- N.A. Lai & J. Fischer. (2012). Efficiencies of power flash cycles. *Energy*, 44(1), 1017-1027.